One site fits both: A model for the ternary complex of folate + NADPH in R67 dihydrofolate reductase, a D_2 symmetric enzyme

Elizabeth E. Howell[a,*], Ushma Shukla[a], Stephanie N. Hicks[a], R. Derike Smiley[a], Leslie A. Kuhn[b,c] & Maria I. Zavodszky[b]

[a]*Department of Biochemistry, Cellular and Molecular Biology University of Tennessee, Knoxville, TN 37996-0840, USA;* [b]*Protein Structural Analysis and Design Laboratory, Department of Biochemistry and Molecular Biology, and* [c]*Center for Biological Modeling, Michigan State University, East Lansing, MI 48824, USA*

Summary

R67 dihydrofolate reductase (DHFR) is a novel enzyme that confers resistance to the antibiotic trimethoprim. The crystal structure of R67 DHFR displays a toroidal structure with a central active-site pore. This homotetrameric protein exhibits 222 symmetry, with only a few residues from each chain contributing to the active site, so related sites must be used to bind both substrate (dihydrofolate) and cofactor (NADPH) in the productive R67 DHFR•NADPH•dihydrofolate complex. Whereas the site of folate binding has been partially resolved crystallographically, an interesting question remains: how can the highly symmetrical active site also bind and orient NADPH for catalysis? To model this ternary complex, we employed DOCK and SLIDE, two methods for docking flexible ligands into proteins using quite different algorithms. The bound pteridine ring of folate (Fol I) from the crystal structure of R67 DHFR was used as the basis for docking the nicotinamide-ribose-P_i (NMN) moiety of NADPH. NMN was positioned by both DOCK and SLIDE on the opposite side of the pore from Fol I, where it interacts with Fol I at the pore's center. Numerous residues serve dual roles in binding. For example, Gln 67 from both the B and D subunits has several contacts with the pteridine ring, while the same residue from the A and C subunits has several contacts with the nicotinamide ring. The residues involved in dual roles are generally amphipathic, allowing them to make both hydrophobic and hydrophilic contacts with the ligands. The result is a 'hot spot' binding surface allowing the same residues to co-optimize the binding of two ligands, and orient them for catalysis.

Abbreviations: R67 DHFR, R67 dihydrofolate reductase; DHF, dihydrofolate; NADPH, nicotinamide adenine dinucleotide phosphate (reduced); NMN, nicotinamide mononucleotide; NOE, nuclear Overhauser effect; ILOE, interligand nuclear Overhauser effect; ITC, isothermal titration calorimetry; Fol I, the productively bound folate fragment (residue D79, from 1VIF); PABA-Glu, para-aminobenzoic acid tail of folate; Protein Data Bank, PDB; NAC, near attack conformer.

Introduction

Dihydrofolate reductase catalyzes the reduction of dihydrofolate (DHF) to tetrahydrofolate using NADPH as a cofactor. This enzyme is essential in folate metabolism since tetrahydrofolate is required for the synthesis of thymidylate, purine nucleosides, methionine, and other metabolic intermediates; thus, DHFR has been a prime target for anticancer and antibacterial therapy. Whereas chromosomal DHFR has been extensively studied and was one of the first successful

*To whom correspondence should be addressed. E-mail: lzh@utk.edu.

targets for structure-based drug design, the plasmid R67 encoded DHFR has only recently been characterized. R67 DHFR is of special interest because it can transfer resistance between bacteria against the antibiotic trimethoprim. This DHFR has an entirely different sequence and fold from chromosomal DHFR [1]. R67 DHFR is a homotetramer in which each short chain forms a five-stranded β-barrel also found in SH3 domains [1] and a variety of other proteins including the Tudor domain of human survival motor neuron protein 1, ferredoxin thioredoxin reductase, nitrile hydratase, two of the 50S ribosomal proteins, and HIV integrase (2; FSSP database at http://www.ebi.ac.uk).

While the mode of ligand binding and catalysis for R67 remains a mystery – to date, only a folate-bound crystallographic complex has been partially characterized [1] – the extensive studies on chromosomal DHFR provide a useful background for studying catalysis by R67 DHFR. Chromosomal DHFR is proposed to be a well-evolved enzyme with a catalytic efficiency of 0.15 [3]. (For comparison, the efficiency for triose phosphate isomerase, which has been described as a 'perfect enzyme', is 0.6 [4].) Hydride transfer rates are faster than the rate-determining step, which is the release of product, tetrahydrofolate [5]. Electrostatic interactions are proposed to steer binding of substrate and cofactor [6]. *Ab initio* quantum mechanical calculations suggest polarization of bound substrate and cofactor occur upon binding, which serves to facilitate hydride transfer [7–10]. A conserved acidic group (Asp in bacterial DHFRs and Glu in mammalian DHFRs) has been variously proposed to be a general acid [11], a mechanism to facilitate raising the N5 pK_a of DHF to 6.5 [12], an electrostatic mechanism to enable enol tautomer formation in DHF [13–14], or a way to polarize bound DHF [15]. Overlapping cofactor and substrate binding sites may help hold the reactants at a distance that facilitates hydride transfer in human DHFR [16]. Finally, dynamics of the protein chain, including subdomain rotation and alternate active site loop conformations, may modulate ligand specificity and catalytic efficiency [17–22]. Chromosomal DHFR binds its ligands with a large enthalpic component through specific interactions [13, 23]. These studies suggest that chromosomal DHFR has developed numerous strategies to maximize catalytic efficiency.

Type II DHFR, typified by R67 DHFR, is a dimer of dimers as shown in Figure 1. The central pore forms the active site, and the high degree of symmetry means that each of the four subunits contributes the same few residues to the binding surface. R67 DHFR is unlike the chromosomal enzyme in another respect. There are three different ligand binding combinations available to its active site: 2 folate/DHF, or 2 NADPH, or 1 folate/DHF plus 1 NADPH [24]. The latter is the productive ternary complex. Thus, each half of the pore can bind either NADPH/NADP$^+$ or folate/DHF, a very different binding strategy than observed for chromosomal DHFR. Crystallographically defining the positions of bound ligands has proven especially difficult for the plasmid encoded enzyme, as the four-fold symmetry within the pore results in a four-fold dilution of the electron density. For example, if one ligand is bound, there is an equal probability that this binding will be in any one of the four equivalent sites within the pore for each of the individual protein copies in the crystal lattice. This effectively dilutes the observed electron density to an average over these four states. The symmetry and small size of the pore also means that the same residues (possibly from different chains) must contribute to the binding of both folate and NADPH. Thus, R67 DHFR is a fascinating system for studying how evolution can select a limited number of residues to co-optimize the catalytically productive binding of two quite different ligands, folate and NADPH.

A previous model of the ternary complex was given in Narayana et al. [1]. However, that model contained three bound ligands (2 folate + 1 NADPH), inconsistent with more recent solution studies indicating only two ligands are bound [24]. Also the model by Narayana et al. positioned the productively bound folate molecule parallel to and above the NADPH molecule. This would predict numerous interligand NOEs, which are not observed in NMR experiments [25]. However, the partial density available for folate in the binary crystallographic complex provides a valuable guide to its favored position within the pore. We evaluated the possibility that NADPH could interact in R67 DHFR in the same orientation relative to folate as it does in the chromosomal DHFR crystal structures. However, due to steric limitations within the pore of R67 DHFR, this binding mode is not feasible. Because the chromosomal DHFR complexes do not explain how the substrate and cofactor bind in R67 DHFR, and this ternary complex has so far proven crystallographically inaccessible, we have used two diverse docking methods to predict their interactions in R67 DHFR. The predicted interaction of NADPH with folate in R67 DHFR is then compared with their
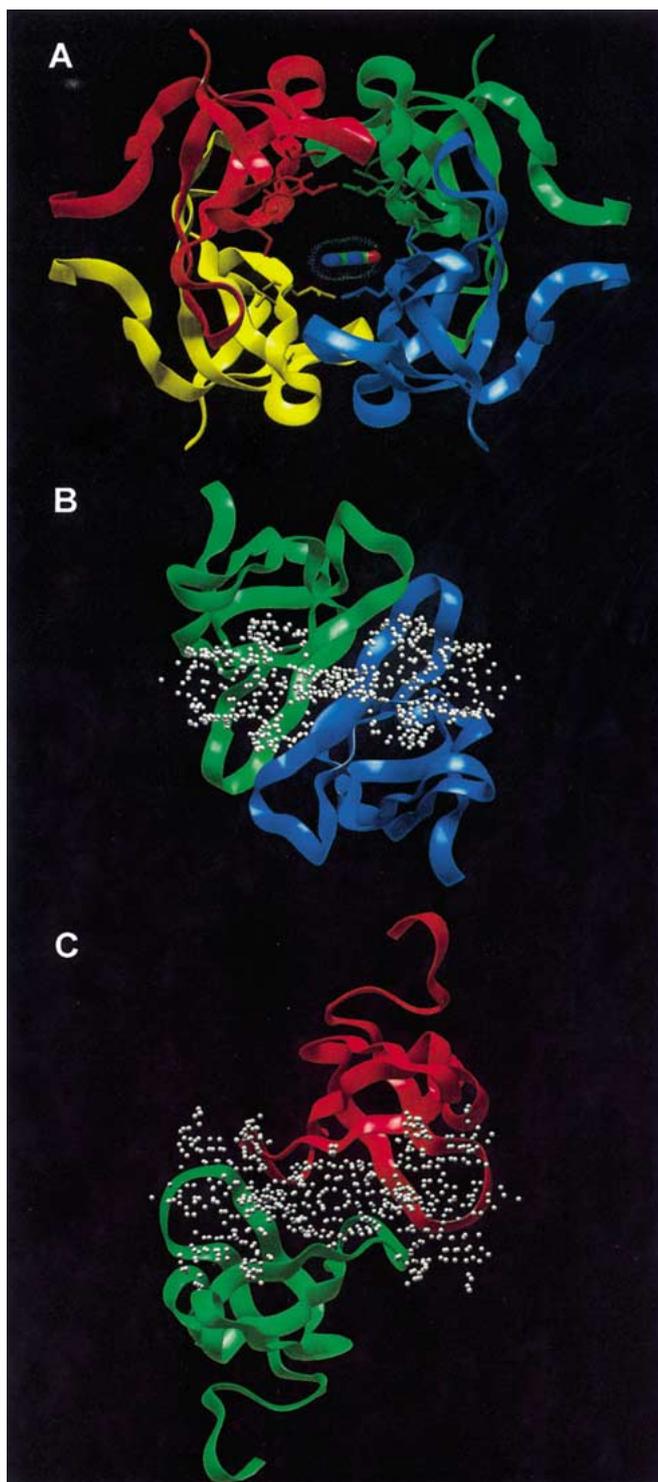
Figure 1. (A) The structure of R67 DHFR is a homotetramer formed by a dimer of dimers in which all four subunits (shown in red, yellow, blue, and green ribbons) contribute equally to create the symmetry related binding sites for folate and NADPH. The pteridine ring of the bound folate (shown in tubes in the central pore) and the side chains of the residues lining the pore are also shown. The view is down a twofold symmetry axis. (B) and (C) describe a reverse image of the active site generated using the SPHGEN subroutine of DOCK on the 1VIE DHFR coordinates from the PDB. Water molecules were removed from the PDB file prior to running SPHGEN. Each sphere point corresponds to a possible atom position for docked ligands. In (A), the sphere cluster would fill the active site pore. Two perpendicular orientations of the protein chains and sphere cluster are shown in (B) and (C).
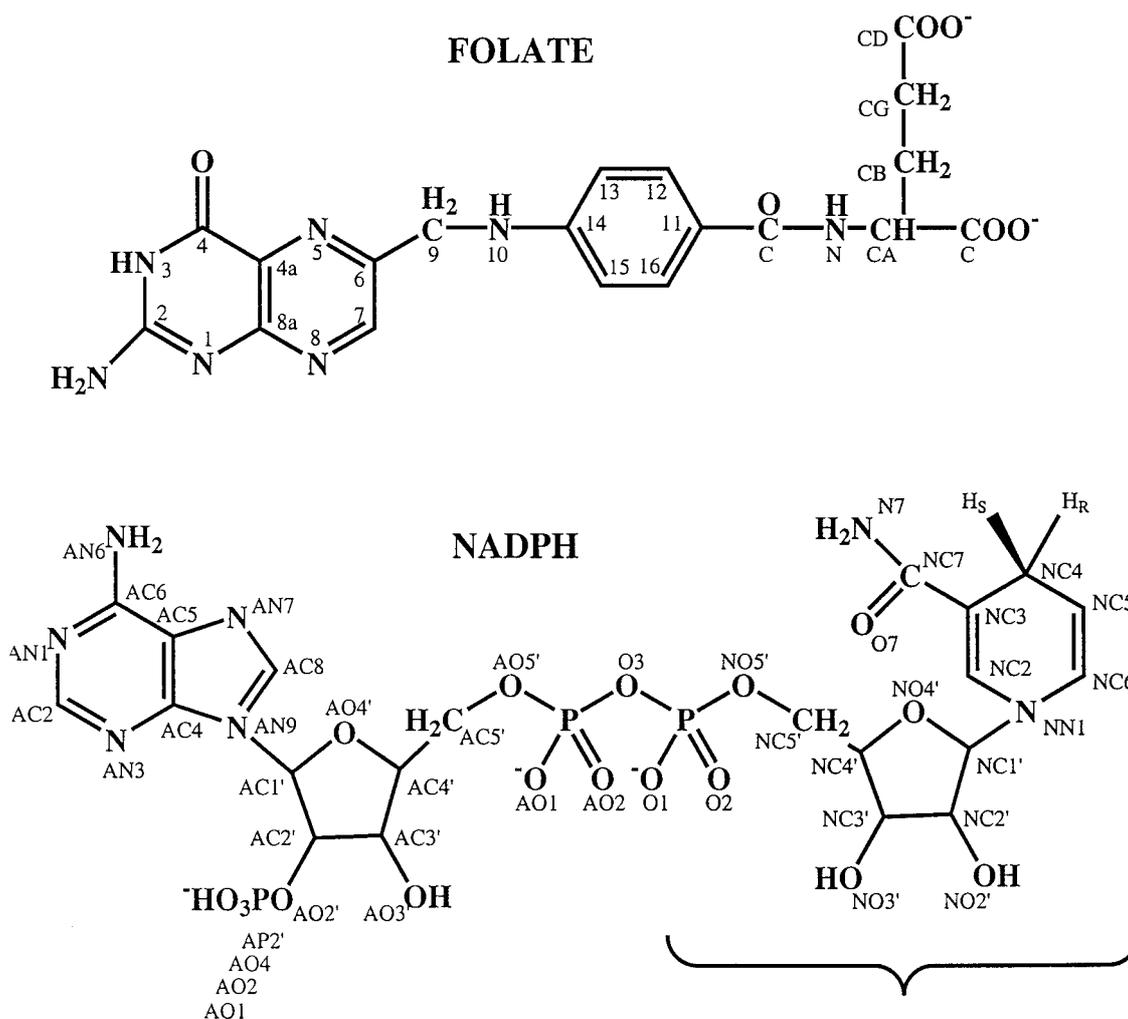
FOLATE

NADPH

Figure 2. The structures of folate and NADPH. Reduction of folate across the C7-N8 bond yields dihydrofolate. During catalysis, the A or *re* hydrogen (H_R) on C4 of the nicotinamide ring faces the *si* face of the folate pteridine ring, which accepts a hydride at C7. The hydride would approach the *si* face of the pteridine ring from beneath the plane of the paper. The NMN moiety of NADPH is indicated by the bracket.

orientation in chromosomal DHFR, and related to the effects of site-directed mutants on ligand binding.

Methods

DOCK v4.0 and SLIDE v1.1 were utilized to predict the binding modes of NADPH and folate in the active-site pore of R67 DHFR. DOCK v4.0 uses van der Waals interactions in its scoring and allows ligand flexibility [26–28]. SLIDE v1.1 includes protein side-chain flexibility, full ligand flexibility, probabilistic inclusion of active-site bound water molecules, and a scoring function with hydrophobic interaction and hydrogen bond terms [29–31]. The structures of folate

and NADPH and their atom labeling conventions are given in Figure 2.

The DOCK v4.0 suite of programs was used to create a reverse image of the active site described by sphere clusters, where each point is a putative atom position for docked ligands. Sphere clusters were generated either for the apo enzyme with all waters removed, or for various ligand complexes described below. A grid surface was calculated for each of these conditions using a Lennard Jones 6–12 potential and a dielectric ratio of 4. The partial charges for DHF or NADPH and its fragments were obtained from Cummins et al. (32; *ab initio* 6-31G*). The partial charges for folate and its fragments were obtained from either the Gasteiger-Huckel subroutine in Sybyl (Tripos)

or from Jennifer Radkiewicz (Old Dominion University, 6-31G*). The flexible ligand option was utilized in DOCK with anchor searching. In this procedure, docking of a rigid, anchor fragment is performed first, followed by stepwise re-building and docking of the rest of the molecule. For NADPH, the minimal anchor size was 6 non-hydrogen atoms while for folate, it was 6 or 10.

DELPHI was used to generate an electrostatic potential surface for R67 DHFR by solving a non-linear Poisson–Boltzman equation [33]. Default settings were used, including 0M salt. The solvent dielectric was 80 and the protein dielectric was set at 2.

CONTACTS (http:/www.dl.ac.uk/CCP/CCP4/html/contact.html) was used to generate the list of contacts between docked structures and R67 DHFR.

SLIDE [29] is a docking/screening tool using distance geometry techniques to dock ligands into the binding site of the target protein via exhaustive matching of all possible ligand anchor fragments to all possible subsets of a template representing the protein binding site. The template points are identified as the most favorable positions for ligand atoms to form hydrogen bonds or make hydrophobic interactions with the neighboring protein atoms. Every combination of three template points is compared to every combination of three ligand interaction points in a search for complementary shape and chemistry, while regions outside the ligand anchor fragment (defined as the part of the ligand bounded by the current three interaction centers) are modeled flexibly. SLIDE is capable of modeling induced complementarity by making adjustments in the protein side chains and ligand upon binding, with the minimal set of necessary rotations determined by mean-field optimization [30]. Each collision-free ligand orientation is scored based on the number of hydrogen bonds and the hydrophobic complementarity with the protein.

CONSOLV, a k-nearest-neighbor-based classifier [34] was used to identify binding-site waters likely to be conserved upon ligand binding based on their mobility and their favorable interactions with the protein. CONSOLV labeled each bound water molecule in the 1VIF R67 DHFR structure according to its probability of being conserved upon ligand binding, and these values were used by SLIDE to appropriately incorporate bound water molecules or to penalize their displacement by non-polar ligand atoms [31].

DRUGSCORE is a knowledge-based scoring function [35] that was shown to discriminate efficiently between well-docked ligand-binding modes

and computer-generated artifacts. We used DrugScore in addition to the built-in scoring function of SLIDE to score and rank all docked ligand orientations with a suitable distance between the C4 atom of the NADPH nicotinamide ring and the C6 of the folate pteridine ring (<5.0 Å).

LIGPLOT [36] was used to create the figures showing the protein-ligand and ligand-ligand hydrogen bonds and hydrophobic interactions.

The coordinates of apo R67 DHFR as well as a binary complex with 2 folates bound are available as 1VIE and 1VIF [1] at the Protein Data Bank (37; http://www.rcsb.org/pdb). In the present study, the structure 1VIF was used. The coordinates of the NADPH molecule were taken from the TRIPOS database for the DOCK experiment. SLIDE handles ligands as flexible molecules, but it avoids large conformational changes compared to the starting conformation. To include a broad range of energetically favorable starting conformations in docking with SLIDE, 59 NADPH molecules were extracted from crystal structures of various protein-NADPH complexes from the PDB. The nicotinamide ring is *syn* with respect to the ribose ring in 14 of these NADPH conformations and it is *anti* in 45 of them.
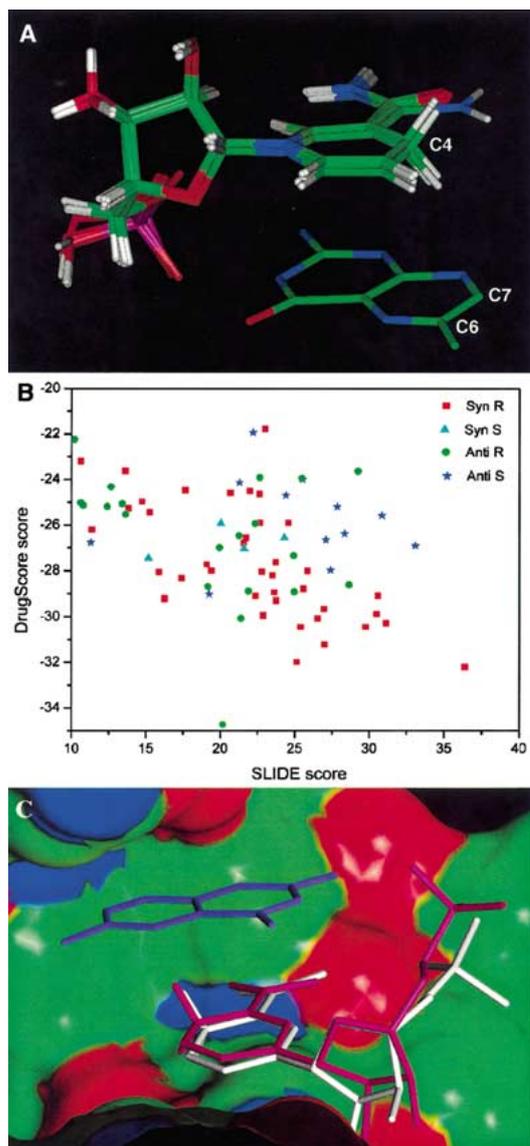
Results

Active site symmetry and docking constraints

A reverse image of R67 DHFR's active site was generated using the DOCK subroutine, SPHGEN. Two orientations of this image, given in Figures 1B and 1C, show the symmetry associated with the pore as well as its size. If the ligand were small with respect to the binding site, four symmetry related sites could potentially be occupied. A larger ligand would reduce the number of possible binding sites because of steric hindrance. Binding of the ligand near the center of the pore, as is the case with Fol I from the crystal structure, is expected to have a similar effect by breaking the 222 symmetry, limiting the number of possible bound molecules to at most two, which is consistent with the experimental results [24].

Several constraints obtained from experimental data were used in preparing the docking experiments and in screening the docked ligand conformations to eliminate unlikely binding modes:

(1) Isothermal titration calorimetry (ITC) data show a total of two ligands bind [24]. The combinations are two folates or 2 NADPHs or 1 NADPH

Figure 3. (A) Orientations of the NMN fragment docked into the R67 DHFR•Fol I sphere cluster using DOCK. The eight top scoring candidates that satisfy the stereochemistry of the reaction (A-side transfer) are shown. The Fol I pteridine fragment was obtained from entry 1VIF in the PDB. Fol I lies at bottom right in the image, while the docked NMN molecules lie at top left. The C4 atom of the nicotinamide ring is labeled, as are the C6 and C7 atoms of the pteridine ring. Atoms are colored according to their chemical properties, with carbon in green; oxygen, red; nitrogen, blue; and hydrogen, white. (B) Comparison of the scores for well docked NMN molecules (consistent with experimental constraints and a distance of less than 5.0 Å between C4 of NADPH and C6 of folate) obtained with two different scoring functions: those of SLIDE and DrugScore. Because the currently available version of DrugScore does not include water-mediated contacts, these dockings did not include water molecules from the binding site, though similar dockings were found with water molecules included. (C) The NMN portion of NADPH docked into the binding site of R67 DHFR in *syn* R orientation next to the pteridine ring of folate (purple, at top). The solvent accessible molecular surface of the binding site [70] is colored according to atom type: carbon is green, oxygen is red and nitrogen is blue. The top scoring orientation of NMN obtained with SLIDE (obtained with the water-mediated template and ranked 1st by SLIDE and 3rd by DrugScore) is shown in white and that obtained with DOCK is shown in magenta. Hydrogen atoms are shown only for the C4 of NADPH, which donates the hydride to reduce folate.

(3) From fitting the electron density, two folate molecules were modeled in asymmetric positions in 1VIF [1]. Fol I is bound productively with its *si* face exposed [38], whereas Fol II has its *si* face against the side of the pore, making it unavailable to receive a hydride. For this reason, Fol I was used to dock NADPH to the binary complex of R67 DHFR-folate.

(4)) For docking of folate or its analogues, the docked pteridine ring should conform to the observed electron density in the crystal structure [1]. This flat density was observed at the center of the pore near the Gln 67 residues, which form the 'floor' and 'ceiling' of the binding site. Density for the *p*-aminobenzoic acid–Glu (PABA-Glu) tail was not observed in the crystal structure, indicating disorder.

Docking to generate a productive ternary complex model using DOCK

Docking of a truncated version of NADPH (NMN) into R67 DHFR•Fol I was initially performed. This corresponds to preliminary electron density maps of bound thio-NADP^{+}, where the nicotinamide ring could be fit, but the tail was disordered (Narayana, personal communication). The docked orientations were visually evaluated by their predicted stereochemistry of hydride transfer. Out of the top 10 docked orientations, eight predicted A-side transfer and two

+ 1 folate. Binding of two NADPH molecules shows negative cooperativity [24], suggesting the first molecule binds at or near the center of symmetry and impedes binding of a second molecule at a symmetry related site. Binding of two folate molecules shows positive cooperativity, indicating there are interactions between the bound folate molecules that enhance affinity.

(2) Interligand NOE (ILOE) data from Li et al. [25] show few ILOE's, suggesting the ligands are bound in extended conformations on opposite sides of the pore and meet somewhere in the middle of the pore.
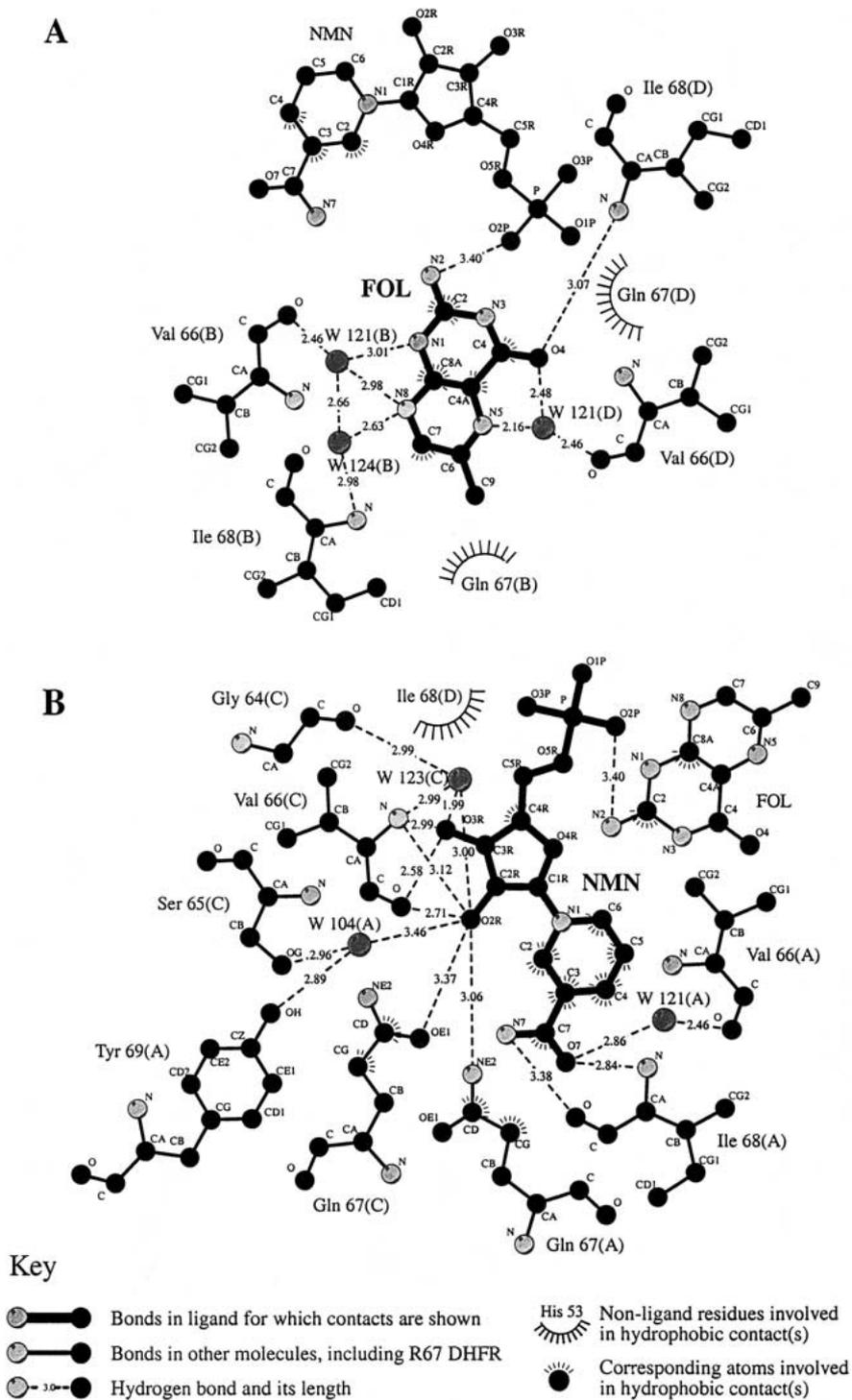
Figure 4. Protein-ligand and ligand-ligand interactions from the R67 DHFR•Fol I•NMN ternary complex for (A) the pteridine ring in the R67 DHFR•Fol I structure and (B) NMN docked in the R67 DHFR•Fol I structure (drawn by LIGPLOT). The position of the NMN molecule in this complex corresponds to the top scoring docking obtained with SLIDE. W denotes water molecules.

predicted B-side transfer. The observed stereochemistry of the R67 DHFR reaction is A side transfer [39]. The eight orientations that predicted A-side transfer were bound on the opposite side of the pore from Fol I. Thus if the PABA-Glu tail of folate and the 2′,5′-ADP tail of NADPH were added back on, these molecules would lie on opposite sides of the pore and minimal ILOEs would be predicted, consistent with the data of Li et al. [25]. In contrast, the two docked NMN conformers that predicted B-side transfer were unlikely candidates, since the nicotinamide ring docked on the same side of the pore as the pteridine ring. Thus, if the PABA-Glu tail of folate and the 2′,5′-ADP tail of NADPH were added back on, these molecules would lie parallel to each other in one half of the pore, and numerous ILOEs would be expected.

The orientations of the eight top scoring candidates from DOCK are shown in Figure 3A. The distance between C4 of the nicotinamide ring and C7 of the pteridine ring required for reduction of folate (a poor substrate) was 3.72–3.93 Å in these dockings. For DHF (assuming it is bound the same way as folate), the distance between C4 of the nicotinamide ring to C6 of the pteridine ring ranged from 4.06–4.30 Å. (These distances are 15–20% ($\sim$ 0.5 Å) longer than the ones seen in a number of known crystal structures of chicken or *E. coli* chromosomal DHFRs complexed with NADP+ and folate or NADP$^+$ and biopterin (1DR1, 1RA2, 1RB2, 1RX2, 7DFR in the protein data bank).) The nicotinamide ring was *syn* with respect to its ribose ring, consistent with the NMR results of Brito et al. [40] and Li et al. [25]. This DOCK run therefore generated a chemically reasonable model for the orientation of the pteridine ring in the R67 DHFR•folate•NMN ternary complex. The RMSD between non-hydrogen atom positions in these dockings ranged from 0.078 to 0.665 Å, indicating a family of substantially similar orientations. Docking of the entire NADPH molecule into the R67 DHFR•Fol I complex was performed next. While the NMN part of the NADPH was docked in the same general area as before, DOCK was not able to predict unambiguously the position of the 2′,5′-ADP tail; a fan of similarly favorable orientations for the ADP tail was observed. Ionic interactions between symmetry related Lys32 residues with either the PP$_i$ bridge or the 2′phospate of NADPH appear important in the various dockings.

Docking of NMN into R67DHFR•Fol I using SLIDE

We analyzed all SLIDE dockings with a distance of 5 Å or less between the C4 of the nicotinamide ring of NMN and the C6 of the folate pteridine ring involved in hydride transfer. There are four possible orientations: the nicotinamide ring can be *syn* or *anti* with respect to its ribose ring, and in both cases either the *pro-R* (A-side) or the *pro-S* (B-side) hydrogen can point toward the pteridine ring. These orientations are named *syn R, syn S, anti R and anti S*, respectively. Among the docked orientations, 39 adopted a *syn R* conformation, 4 were in *syn S*, 20 in *anti R*, and 12 in *anti S*. This distribution indicated a preference for the *syn* R orientation of NMN to interact with the R67 DHFR-Fol I complex, especially given that there were about three times as many *anti* conformers as *syn* conformers in the input data set of NADPH molecules. The *syn R* orientation is the one most consistent with the experimental results [25, 39].

In addition to the built-in scoring function of SLIDE, DrugScore [35] was used to evaluate these NMN dockings. DrugScore calculates an empirical intermolecular potential, with the best scores having the largest negative values, whereas the best SLIDE scores have the largest positive values (greater hydrophobic complementarity and number of intermolecular hydrogen bonds). Most of the high-scoring ligand orientations (lower right in Figure 3B) were in *syn* conformation with the *R*-side hydrogen of the nicotinamide ring directed toward the folate. These orientations had the best scores with both scoring functions, except for one *anti R* orientation, which obtained an unusually high score with DrugScore. The available version of DrugScore does not consider water-mediated interactions, and therefore preferred dockings of NADPH closest to the wall of the binding site such as this one. The *anti S* orientations, which obtained high scores from SLIDE but not DrugScore, had a larger number of hydrogen bonds formed between the P$_i$ of NMN and various protein residues, but the nicotinamide ring formed at most one hydrogen bond with the protein. However, to have a well-defined stereochemistry between NADPH, folate, and the protein, some specific hydrogen bonding is expected between the head of the NADPH molecule and DHFR. The docked NMN in *syn R* orientation best fulfills this requirement by forming three hydrogen bonds between the O7 and N7 atoms of the nicotinamide head and the backbone oxygen and nitrogen of Ile 68, as well as the backbone

oxygen of Val 66, the latter being mediated by a water molecule (W 121A).

For waters bound in the DHFR•Fol I crystallographic complex, CONSOLV [33] was used to predict their probability of conservation upon NADPH binding, based on the favorability of their interactions with the protein. After eliminating those water molecules that were found to be too close (<2.5 Å) to a protein or folate atom, only 11 water molecules were predicted to be more than 50% likely to be conserved inside the pore. Performing the docking experiment with the conserved water molecules included as part of the binding site did not result in significantly different dockings. The preference for the *syn R* orientation of the docked NMN was slightly higher compared to the dockings without waters, accounting for 62% of the docked conformations that have a high SLIDE ranking.

A number of water molecules were found to be important in anchoring the docked NMN to the protein (Figure 4B), similarly to water molecules 121 and 124 (Figure 4A) which have been suggested to form a bridge between the pteridine ring of folate and the backbone of the R67 DHFR [1]. However, these water molecules were predicted to be only moderately conserved by CONSOLV. The explanation of this finding originates in the symmetry of the binding site: the productively bound pteridine ring can occupy any of the four symmetry related positions in the R67 DHFR tetramer structure, and by doing so it displaces different water molecules in different tetramers in the crystal lattice. As a result, many water molecules from the crystal structure of the R67 DHFR-folate complex (PDB entry 1VIF) have high temperature factors. In predicting conserved waters, CONSOLV weighs temperature factors heavily, so most of these waters were predicted to be only 28–55% conserved.

There is a good agreement between the predictions of SLIDE and DOCK: both predict *syn R* to be the most likely orientation of the NMN molecule relative to folate. The position of the nicotinamide ring in the top scoring orientations (using SLIDE's scoring function) *syn R* is very similar to the top orientation produced using DOCK (Figure 3C). The largest differences are found in the position of the P_i group of NMN, which is understandable given the large space available and the absence of constraints because of the missing tail of the NADPH. The non-hydrogen atom RMSD between the top NMN orientations obtained with DOCK and SLIDE is 1.5 Å (Figure 3C). The SLIDE scores and DrugScore scores for these two top dockings are 28.8 and −34,1300 for the DOCK docking and 36.4 and −32,2246 for the SLIDE docking.

The protein-ligand interactions generated by LIG-PLOT [36] for the R67 DHFR•Fol I•NMN ternary complex are shown in Figures 4A and 4B for the pteridine ring and NMN respectively. The position of the NMN molecule corresponds to the top scoring NMN docking obtained with SLIDE, and the Fol I position from the crystal structure is used. Contacts between the dockings and the protein-ligand binary complexes used as docking targets are listed in detail in the Supplementary Material (Tables 1–3). A comparison of the contacts for NMN and folate shows that symmetry related residues were involved in binding both ligands. For example, Gln 67 from both the B and D subunits made several contacts with the pteridine ring, while Gln 67 from the A and C subunits made several contacts with the nicotinamide ring. Utilization of symmetry related residues during binding was also observed for Ile 68. Fol I binding involved Ile 68 from the D subunit which interacted with the pteridine ring, while Ile 68 from the A and D subunits interacted with the nicotinamide and ribose groups. Numerous van der Waals contacts and a hydrogen bond were also predicted between the ligands, as shown in Figures 4A and 4B. Positive cooperativity has been previously observed between R67 DHFR•NADPH and DHF [24]. The proposed interactions between NMN and Fol I may describe how positive cooperativity between NADPH and folate is generated.

One of the significant differences between SLIDE and DOCK is that SLIDE allows protein flexibility upon docking by balancing ligand and protein side chain rotations to resolve van der Waals overlaps. In the case of R67 DHFR, there were only slight movements of two Gln 67 residues from subunits A and C, resulting in displacements of less than 0.5 Å away from the docked NMN molecule, maintaining the original hydrogen-bonding pattern of the protein.

Docking of folate into R67 DHFR•NMN Using DOCK

As a next step towards evaluating how the complete folate molecule (much of which is not resolved in the crystal structure) might bind in the ternary complex, the top scoring A-side NMN conformer (Figure 3A) was used to generate a sphere cluster and folate was docked into this complex. If the R67 DHFR•NMN•folate interactions were unique,

1044

Table 1. A comparison of steady state kinetic values for R67 DHFR variants at pH 7.0

DHFR Species	k_{cat} (s^{-1}) (pH 7)	$K_{m(DHF)}$ (μM)	$K_{m(NADPH)}$ (μM)
Wt R67 DHFR[a]	1.3 ± 0.07	5.8 ± 0.02	3.0 ± 0.06
S65A R67 DHFR[b]	1.1 ± 0.10	4.0 ± 0.51	2.9 ± 0.57
Q67H R67 DHFR (pH 8)[c]	0.022 ± 0.003	0.16 ± 0.01	0.028 ± 0.001
I68M R67 DHFR[b]	0.17 ± 0.03	25 ± 3.0	21 ± 3.0
Y69F R67 DHFR[b]	2.5 ± 0.04	44 ± 2.1	66 ± 2.6

[a] Values from reference 62.
[b] Values from reference 54.
[c] Values from reference 52.

the pteridine ring of folate would be expected to dock in a similar orientation as Fol I. Out of the top 25 scoring orientations, 21 place the pteridine ring of folate in the same general position as Fol I. Two others flip the pteridine ring 180° so that the correct *si* face is shielded against the protein surface and is unavailable to accept a hydride, and two bind on the same side of the pore as the NADPH fragment. The latter would predict numerous ILOEs, which are not observed.

The position of the PABA-Glu tail of folate was observed to vary in these dockings, consistent with the disorder predicted by the electron density in the crystal structure. In addition, the ILOE results of Li et al. [25] indicate the Glu tail of folate is disordered. Figure 5 shows the top 21 docked conformers. The contacts generated by the top scoring conformer are given in Table 2 of the Supplementary Material. When the interactions are compared, it is again clear that similar residues are implicated in binding both NMN/NADPH and folate: Gln 67, Lys 32, Val 66, Ile 68 and Tyr 69.

As expected, given the insensitivity of current docking algorithms to very small differences in chemistry, docking DHF (where the C7-N8 bond of folate in Figure 2 is reduced) produced similar results to the folate dockings. While the pteridine rings docked in the same general area, the PABA-Glu tails showed variability in their positions (results not shown). The distance between C4 of the nicotinamide ring to C6 of the pteridine ring involved in hydride transfer ranges from 4.45–6.07 Å. In some dockings, an ionic interaction was predicted between the carboxylate termini of the Glu tail and Lys 32 of the C subunit, whereas others showed the carboxylate of the Glu tail interacting with Lys 32 of the B subunit. Thus, symmetry related Lys 32 residues could stabilize DHF binding in two different orientations.

Comparison of the positions of Fol I from the crystal structure with the pteridine rings of the highest-scoring docked folate and DHF conformers show heavy-atom RMSDs of 3.6 and 4.2 Å, respectively. While this reflects slight differences in position, the binding modes are clearly related, indicating DOCK can predict the Fol I binding mode reasonably well starting with docked NMN.

Electrostatic potential calculations

An electrostatic potential surface for R67 DHFR was generated using DELPHI, which solves the non-linear Poisson–Boltzman equation [33]. Although no charged residues penetrate deeply into the active site pore, DELPHI predicts that R67 DHFR possesses a positively charged active site pore (Figure 6). This charge originates from the nearby residues, Lys 32 and Lys 33, as computational mutation of these residues to methionine results in a predicted loss of the positively charged active site. This positive potential is likely attractive to the two negatively charged ligands, folate and NADPH (NADPH has a net charge of −3 while folate/DHF has a net charge of −2), whereas the net negative charge on the outside of the torus may aid in electrostatic guidance. This prediction is consistent with the docking results that Lys 32 can form ionic interactions with the negatively charged tails of folate and NADPH. Lys 32 resides on the outer edge of the active site pore, while Lys 33 is exposed on the surface of the protein.
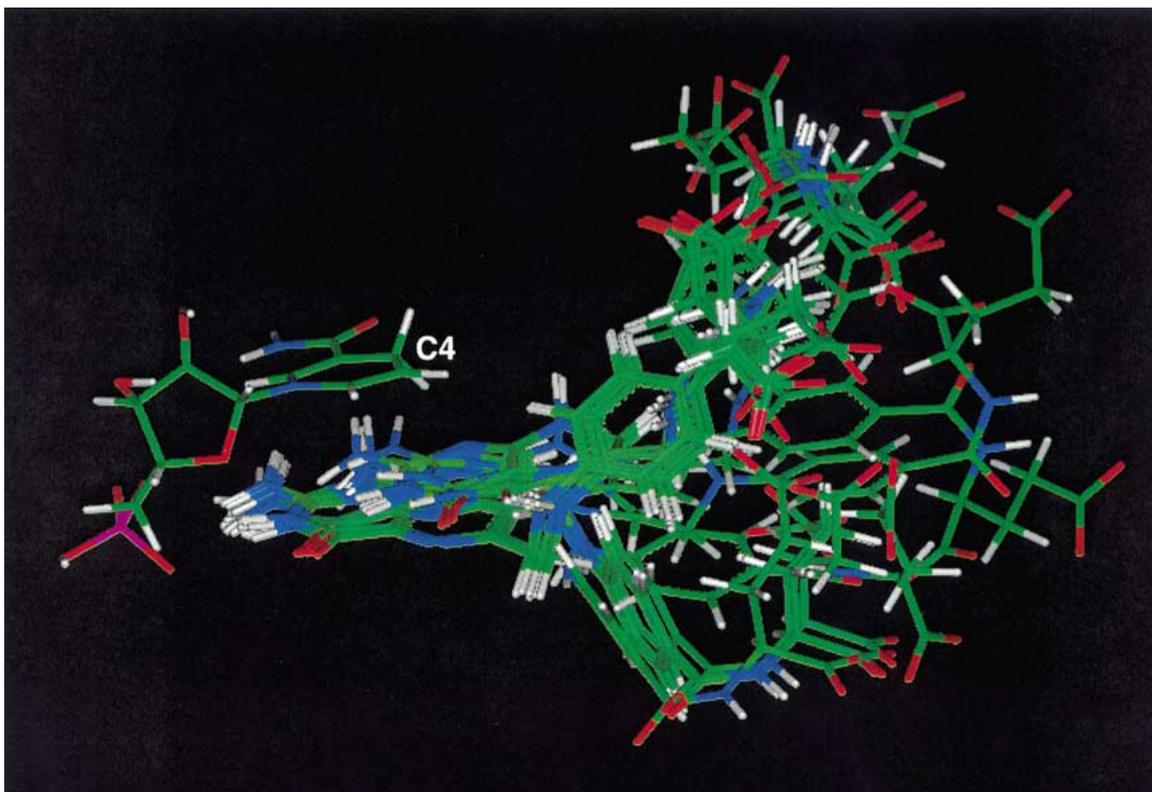
Figure 5. Orientations of folate docked into the R67 DHFR•NMN sphere cluster using DOCK. The NMN conformer used in generating the sphere cluster was the top scoring candidate from Figure 3A. The docked folate candidates were evaluated based on their ability to predict the correct reaction stereochemistry. The pteridine ring docks fairly consistently in a position that is similar to that of Fol I in the crystal structure, while the PABA-Glu tail has numerous potential orientations. NMN lies at top left with the superimposed folate dockings shown on the right. The C4 atom of the nicotinamide ring is labeled.

Discussion

How can R67 DHFR bind both NADPH and folate?

There are a number of cases in which the same site in a protein is designed to accommodate binding of several different ligands. Binding of diverse peptides to the major histocompatibility complex is achieved by having a number of specific binding pockets available for different side chains as well as by making key interactions to the peptides' backbones [41–42]. Binding of different unfolded protein chains to GroEL is proposed to be accomplished mainly by hydrophobic interactions where more flexibility is allowed [43]. To bind various sugars, the maltodextrin transport/chemosensory receptor uses aromatic rings to interact with the sugar ring faces [44]. Binding of various peptides to oppA, a peptide transporter, utilizes numerous intermediary water molecules [45], as does binding of various fatty acids to adipocyte lipid-binding protein [46], binding of various sugars to

arabinose binding protein [47], and high-affinity binding of a proteinaceous inhibitor, BLIP, to β-lactamases with diverse sequences [48]. These are all mechanisms to facilitate numerous binding modes.

Hot spots for protein-protein interactions have been noted and evaluated by mutagenesis and statistical analysis [49–51]. A general trend proposed is the presence of residues that are amphipathic or can make hydrophobic and hydrogen-bonding interactions. For example, Tyr, Trp and Arg have a large hydrophobic component to their side chains as well as the ability to provide polar interactions. The residues that provide binding contacts in the center of R67 DHFR's active site pore include Ser 65, Val 66, Gln 67, Ile 68 and Tyr 69. The side chains of Ser 65 and Gln 67 are polar, while those of Val 66 and Ile 68 are hydrophobic. However, since Val 66 and Ile 68 present both their hydrophobic side chains as well as their backbone NH- and carbonyl groups for potential interactions, they can mediate both hydrophobic and polar interactions
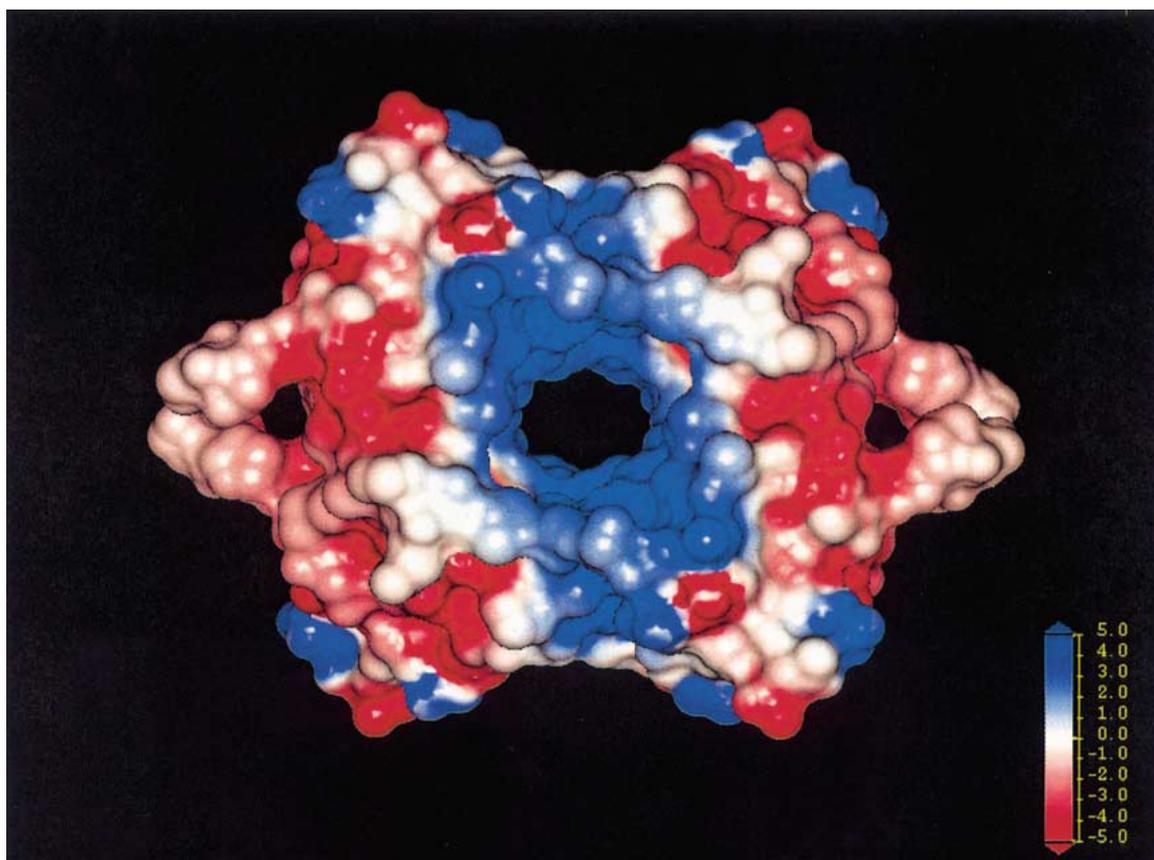
1046

Figure 6. An electrostatic potential surface generated for R67 DHFR by DELPHI. The active site pore is seen in the middle of the structure. Shades of blue describe levels of positive charge while shades of red describe levels of negative charge. Neutral areas are colored white. The charge icon at lower left correlates the color intensity with the potential in kT units.

on the active site pore surface. Similarly, the side-chain methylene groups of Gln 67 also comprise part of the binding surface.

From Figures 4A and 4B (as well as tables in Supplementary Material), it is clear that the same residues are likely to be involved in binding both NADPH/NMN and folate/DHF. Utilization of protein symmetry is the mechanism by which this is achieved. For example, Gln 67 from subunits A and C make contacts with the NMN moiety while Gln 67 from sub-units B and D make contacts with folate. This trend is also apparent with Val 66, Ile 68, Tyr 69 and Lys 32 residues. When symmetry operations are performed on the docked folate and NMN conformers, it is clear that while the binding sites are not identical, they overlap to a great extent. Three of the four symme-try related sites (generated by symmetry rotations) are shown in Figure 7. Two of the symmetry related sites compare the Fol I and NMN (top scoring conformer

from DOCK) binding modes while the third compares NMN and Fol II (the non-productively bound folate in 1VIF). The fourth symmetry related site is empty, pre-cluding a comparison. Polar atoms that occupy similar positions in panel A are N5 of Fol I and N1 of the nicotinamide ring of NMN. In panel B, the C4 oxygen (Fol I) and the carboxamide oxygen (NMN), the N1 (Fol I) and N1 (NMN) as well as the N3 (Fol I) and carboxamide nitrogen (NMN) atoms occupy similar positions. Finally in panel C, the corresponding pairs of polar atoms that are close in space include: the C4 oxygen (Fol II) and the carboxamide oxygen (NMN) as well as the N1 (Fol II) and the N1 (NMN) atoms. This comparison supports a variation of hot spot bind-ing, in which a few residues are responsible for most of the binding through making both polar and hydropho-bic interactions with a small molecule ligand, rather than a protein [49].
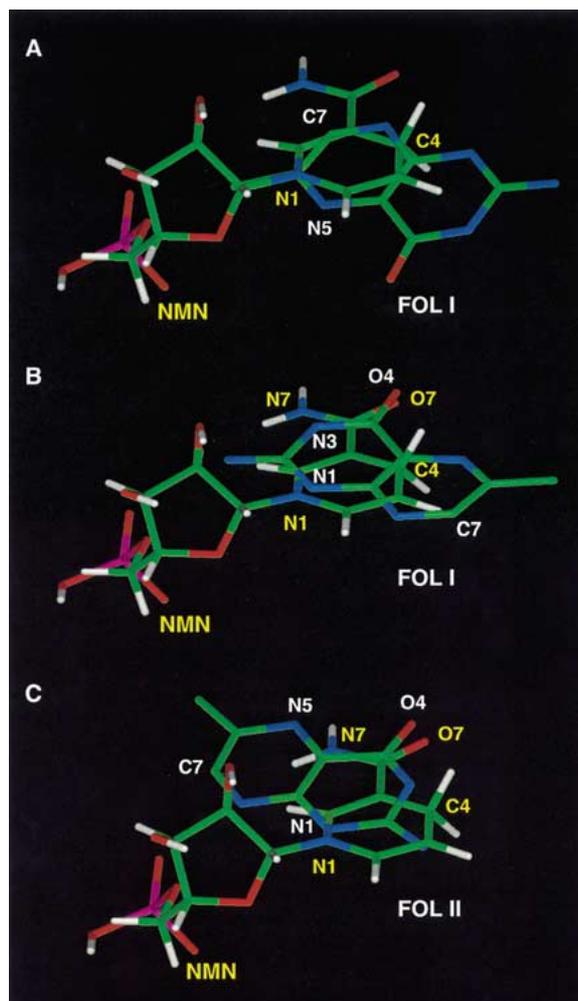
Figure 7. Overlap of the NMN binding site with Fol I and Fol II sites. While two molecules do not bind in the same site concurrently, the symmetry of R67 DHFR implies that the same site must be used at different times for both NADPH and folate (in different halves of the pore or in different copies of the protein). Here, the top-scoring orientation of NMN from DOCK (Figure 3A) is compared (by symmetry operations) with the crystallographic orientation of Fol I or Fol II in the same site. Their substantial overlap corresponds to the region in which residues must be co-optimized for NADPH and folate binding. NMN atoms are labeled in yellow while Fol I or Fol II atoms are shown in white. In (A), the closest protein atoms for interaction with the N1 (NMN) and N5 (Fol I) nitrogens are the carboxamide groups of the Q67 residues (3.69–4.46 Å distant). In (B), the closest protein atoms for interaction with the N1 ligand nitrogens are again the Q67 carboxamide groups (3.68–3.93 Å). For interaction with the O4 (Fol I) or O7 (NMN) oxygens, the backbone NH from I68 lies nearby (3.07–3.25 Å). The N3 (Fol I) or N7 (NMN) atoms come closest to the backbone oxygen of I68 (3.57–4.75 Å). In (C), the backbone NH of I68 is close (2.90–3.25 Å) to the O4 (Fol II) or O7 (NMN) oxygens while the backbone oxygen of I68 could interact with the N5 (Fol II) or the N7 (NMN) atoms (2.68–3.28 Å). The closest protein atoms for interaction with the N1 nitrogens are again the carboxamide groups from the Q67 pairs (3.68–4.37 Å). A similar comparison of the overlap between the Fol I and Fol II sites is shown in Figure 4b of Narayana et al. [1].

The number of similar docking orientations of the NMN fragment of NADPH indicates some alternative possibilities for hydrogen bonding to DHFR. This is also consistent with some mobility of bound NADPH, which in turn may explain the lower catalytic efficiency of R67 DHFR. Because of the high degree of symmetry associated with the binding site of R67 DHFR, the catalytically productive folate•NADPH complex can bind in four equivalent positions, such that both molecules can be positioned at either side of the pore. The position adopted by NADPH independent of folate might well be different from the optimal position when folate is present, for two reasons: because folate creates a new chemical and structural environment that can favor a different placement of NADPH, and because the symmetry of the pore tells us

that there may be several favored, overlapping optimal placements for folate and NADPH (Figure 7). Therefore, it seems that co-optimization of both ligands' binding is important.

Relationship to mutagenesis results

Mutagenesis of R67 DHFR has been performed to evaluate the roles of many of the pore residues in ligand binding: Lys 32, Ser 65, Gln 67, Ile 68 and Tyr 69 [52–54]. The effects of mutations are consistent with the docked interactions of NADPH and folate (Figure 4). Lys 32 was predicted by DELPHI and docking studies to generate favorable electrostatic interactions with the ligands. However, mutations at Lys 32 disrupt the tetramer, so the effects of this side chain on ligand binding cannot be evaluated by mutagenesis. Mutating Ser 65 to Ala does not affect catalytic efficiency, suggesting it does not interact directly with the ligands. NMN docking by SLIDE predicted the Ser 65 side chain hydrogen bonds to a water molecule that participates in NMN binding; however, this water site is also stabilized by interactions with Tyr 69 and could persist in the absence of interactions with Ser 65. Gln 67 hydrogen bonds directly with NMN and makes hydrophobic interactions with folate in the docked ternary complex. Ile 68 makes direct hydrogen bond and hydrophobic interactions with NMN, as well as water-mediated interactions with folate. Tyr 69 participates in water-mediated interactions with NMN. As shown in Table 1, mutations at any of these residues (except S65) alter the K_m values for both ligands. The changes in K_m vary over three orders of magnitude (from 100 fold tighter to 10-fold weaker), however the ability of the mutations to preferentially alter NADPH vs. DHF binding appears marginal [52, 54]. These data support a dual role for these active-site residues in binding both ligands.

Electrostatic interactions

The docking results for full length folate/DHF and NADPH predict that K32 can form an ionic interaction with the 2′ phosphate group in NADPH as well as either of the carboxylate groups in folate/DHF, depending on which ligand occupies the half-pore. This is facilitated by two symmetry related Lys 32 residues at each end of the pore, which allow several different interactions. This may facilitate alternate binding modes or increase the avidity. In addition, the electrostatic potential calculated by DELPHI predicts a positive potential within the pore generated by the Lys 32 and Lys 33 residues, which can serve to electrostatically guide negatively charged ligands. R67 DHFR prefers NADPH as a cofactor over NADH; when NADH is used, a 21-fold elevation in K_m and a 17-fold reduction in k_{cat} are observed when compared to NADPH usage [55]. This also suggests that stabilizing interactions between the additional 2′ phosphate in NADPH with the positive environment within the pore contribute to catalysis.

Electrostatic interactions have previously been proposed in *E. coli* chromosomal DHFR and involve positioning of Lys 32, Arg 52 and Arg 57 near the folate binding pocket and Arg 44, Lys 76 and Arg 98 near the NADPH binding pocket. Arg 44 in chromosomal DHFR from *L. casei* forms a salt bridge with the carboxylate termini of the PABA-Glu tail as monitored by NMR [56] and is important in binding NADPH in *E. coli* DHFR by site-directed mutagenesis studies [57]. The other residues have been proposed to generate a positively charged electrostatic potential in order to attract the negatively charged folate and NADPH molecules to the active site [6].

A model for hydride transfer

The pteridine ring•NMN model shown in Figure 3A predicts hydride transfer distances of 3.72–3.93 Å between C7 of the pteridine ring and C4 of the nicotinamide ring, which participate in the reduction of folate. The best Fol I (pteridine ring)•NADPH docking predicts a hydride transfer distance of 4.63 Å for reduction of folate. The folate•NMN model in Figure 5 predicts distances of 3.66–5.32 Å. For the DHF•NMN model, the distance varies between 3.66–5.24 Å. All these distances are longer than the 2.6–2.7 Å predicted by *ab initio* calculations [58, 59] and from a model of the transition state in *E. coli* DHFR [60]. No docking method would probably be able to reproduce the distances predicted by *ab initio* calculations for transition state complexes, but it is possible to reproduce crystal structure orientations with differences in intermolecular distances of approximately 0.2 Å. When testing the capacity of SLIDE to reproduce the crystal structure orientation of NADP$^+$ from a chromosomal DHFR in complex with folate and NADP$^+$ (PDB code 1RA2), the docked orientation of NADP$^+$ closest to the crystal structure position resulted in a C4–C7 distance of 3.45 Å, comparable to the 3.21 Å value found in that same crystal structure. The greater distances observed in the R67 DHFR dockings imply either a low rate of

hydride transfer or an interligand chemical attraction that shortens the distance.

A recent review by Bruice and Benkovic [61] discusses the relationship between the geometry of bound ligands (near attack conformers or NACs) and catalytic efficiency (k_{cat}/K_m). NACs resemble the transition state and facilitate the formation of a chemical transition state. In particular, molecular dynamics suggests a relationship between catalytic efficiency and close contact distance between the reactive groups. The longer equilibrium hydride transfer distances predicted from the above docking studies suggest why R67 DHFR is not a very efficient enzyme when compared to chromosomal DHFR. The rate-determining step in R67 DHFR is hydride transfer, with a rate of 1.3 s^{-1} at pH 7 [62]. In contrast, the rate determining step in *E. coli* chromosomal DHFR is release of product, and the hydride transfer rate is 238 s^{-1} [4, 63]. The endo conformer predicted by Andres et al. [64] for the reduction of DHF is consistent with the geometry between the pteridine and nicotinamide rings in R67 DHFR, as predicted by the docking calculations and by the ILOEs monitored by Li et al. [25]). The constraints on the active site pore of R67 DHFR are quite clearly different than those in *E. coli* chromosomal DHFR.

Molecular dynamic studies suggest that in general, enthalpic contributions to catalysis predominate over entropic contributions (see Bruice & Benkovic review and references therein, [61]). However in R67 DHFR, a range of similar docking modes is predicted for the ligands, or perhaps an unusual degree of mobility. Both these options likely result from the use of symmetry related residues. The ability of the PABA-Glu tail of folate and the 2′,5′-ADP tail of NADPH to remain flexible but still maintain favorable electrostatic interactions may enhance binding through entropic as well as enthalpic contributions. An additional consequence of alternate binding modes for the ligand tails (or an enhanced mobility) might be to prevent binding of two molecules in one half of the pore, and instead steer binding to one molecule in opposite sides of the pore.

Conclusions

The evolution of catalytic activity is the focus of many recent research articles. One perspective suggests new enzymes evolve by gene duplication followed by accumulation of mutations. This approach takes advantage of structural and mechanistic similarities in generating different catalytic activities and suggests a certain level of catalytic promiscuity [65, 66]. In addition, catalytic antibodies might be expected to provide insight into the process of enzyme evolution. They appear to adopt predominately a lock and key strategy towards binding transition state analogs. Also, a comparison of different catalytic antibodies that catalyze the same reaction suggests they mostly converge to the same binding site motif [67, 68 and references in both reviews; 69]. In contrast to these evolutionary strategies, the results of DOCK and SLIDE showing the favored orientation of NADPH relative to folate in R67 DHFR indicate this enzyme has adopted a novel, yet simple approach: the utilization of symmetry related residues to bind both NADPH/NADP$^+$ and folate/DHF using a range of interaction types through a limited number of amphipathic residues. This symmetry is used to generate a hot-spot surface that accommodates numerous, different interactions, including electrostatic guidance of the ligands.

Electronic supplementary material

Three tables listing the predicted contacts between R67 DHFR•Fol I and docked NADPH, between R67 DHFR•NMN and docked folate (highest scoring conformer) and between R67 DHFR•NMN and docked dihydrofolate (highest scoring conformer) are given. These models were constructed using DOCK.

Acknowledgements

References

1. Narayana, N., Matthews, D.A., Howell, E.E. and Xuong, N.H., Nat. Struct. Biol., 2 (1995) 1018.
2. Holm, L. and Sander, C., Science, 273 (1999) 595.
3. Fierke, C.A., Kuchta, R.D., Johnson, K.A. and Benkovic, S.J., Cold Spring Harbor Symp. Quant. Biol., 52 (1987) 631.
4. Albery, W.J. and Knowles, J.R., Biochemistry, 15 (1976) 5631.

5. Fierke, C.A., Johnson, K.A. and Benkovic, S.J., Biochemistry, 26 (1987) 4085.

6. Bayorath, J., Kitson, D.H., Kraut, J. and Hagler, A.T., Proteins 11 (1991).

7. Bayorath, J., Kitson, D.H., Fitzgerald, G., Andzelm, J., Kraut, J. and Hagler, A.T., Proteins, 9 (1991) 217.

8. Bayorath, J., Kraut, J., Li, Z., Kitson, D.H. and Hagler, A.T., Proc. Natl. Acad. Sci. USA, 88 (1991) 6423.

9. Bayorath, J., Li, J.Z., Fitzgerald, G., Kitson, D.H., Farnum, M., Fine, R.M., Kraut, J. and Hagler, A.T., Proteins, 11 (1991) 263.

10. Greatbanks, S.P., Gready, J.E., Limaye, A.C. and Rendell, A.P., Proteins, 37 (1999) 157.

11. Howell, E.E., Villafranca, J.E., Warren, M.S., Oatley, S.J. and Kraut, J., Science, 231 (1986) 1123.

12. Chen, Y.Q., Kraut, J., Blakley, R.L. and Callender, R., Biochemistry, 33 (1994) 7021.

13. Lee, H., Reyes, V.M. and Kraut, J., Biochemistry, 35 (1996) 7012.

14. Cannon, W.R., Garrison, B.J. and Benkovic, S.J., J. Am. Chem. Soc., 119 (1997) 2386.

15. Casarotto, M.G., Basran, J., Badii, R., Sze, K.H. and Roberts, G.C.K., Biochemistry, 38 (1999) 8038.

16. Davies, J.F. II, Delcamp, T.J., Prendergast, N.J., Ashford, V.A. Freisheim, J.H. and Kraut, J., Biochemistry, 29 (1990) 9467.

17. Farnum, M., Magde, D., Howell, E.E., Hirai, J.T., Warren, M.S., Grimsley, J.K. and Kraut, J., Biochemistry, 30 (1991) 11567.

18. Sawaya, M.R. and Kraut, J., Biochemistry, 36 (1997) 586.

19. Miller, G.P. and Benkovic, S.J., Chem. Biol., 5 (1998) R105.

20. Radkiewicz, J.L. and Brooks, III C.L., J. Am.. Chem. Soc., 122 (2000) 225.

21. Pan, H., Lee, J.C. and Hilser, V.J., Proc. Natl. Acad. Sci. USA, 97 (2000) 12020.

22. Jacobs, D.J., Rader, A.J., Kuhn, L.A. and Thorpe, M.F., Proteins, 44 (2001) 150.

23. Filman, D.J., Bolin, J.T., Matthews, D.A. and Kraut, J., J. Biol. Chem., 257 (1982) 13663.

24. Bradrick, T.D., Beechem, J.H. and Howell, E.E., Biochemistry, 35 (1996) 11414.

25. Li, D., Levy, L.A., Gabel, S.A., Lebetkin, M.S., DeRose, E.F., Wall, M.J., Howell, E.E. and London, R.E., Biochemistry, 40 (2001) 4242.

26. Kuntz, I.D., Blaney, J.M., Oatley, S.J., Langridge, R. and Ferrin, T.E., J Mol Biol., 161 (1982) 269.

27. Shoichet, B.K. and Kuntz, I.D., Prot. Eng., 6 (1993) 723.

28. Ewing, T.J.A. and Kuntz, I.D. J. Comp. Chem., 18 (1997) 1175.

29. Schnecke, V., Swanson, C.A., Getzoff, E.D., Tainer, J.A. and Kuhn, L.A., Prot. Struct. Funct. Genet., 33 (1998) 74.

30. Schnecke, V. and Kuhn, L.A., Intell. Syst. Mol. Biol., (1999) 242.

31. Schnecke, V. and Kuhn, L.A., Persp. Drug Disc. Des., 20 (2000) 171.

32. Cummins, P.L., Ramnarayan, K., Singh, U.C. and Gready, J.E., J. Am. Chem. Soc., 113 (1991) 8247.

33. Honig, B. and Nicholls, A., Science, 268 (1995) 1144.

34. Raymer, M.L., Sanschagrin, P.C., Punch, W.F., Venkataraman, S., Goodman, E.D. and Kuhn, L.A., J. Mol. Biol., 265 (1997) 445.

35. Gohlke, H., Hendlich, M. and Klebe, G., J. Mol. Biol., 295 (2000) 337.

36. Wallace, A.C., Laskowski, R.A. and Thornton, J.M., Prot. Eng., 8 (1995) 127.

37. Berman, H.M., Westbrook, J., Feng, Z., Gilliland, G., Bhat, T.N., Weissig, H., Shindyalov, I.N. and Bourne, P.E., Nucl. Acids Res., 28 (2000) 235.

38. Charlton, P.A. and Young, D.W., J. Chem. Soc. Perkins Trans I (1985) 1349.

39. Brito, R.M.M., Reddick, R., Bennett, G.N., Rudolph, F.B. and Rosevear, P.R., Biochemistry, 29 (1990) 9825.

40. Brito, R.M.M., Rudolph, F.B. and Rosevear, P.R., Biochemistry, 30 (1991) 1461.

41. Matsumura, M., Fremont, D.H., Peterson, P.A. and Wilson, I.A., Science, 257 (1992) 927.

42. Fremont, D.H., Matsumura, M., Stura, E.A., Peterson, P.A. and Wilson, I.A., Science, 257 (1992) 919.

43. Chen, L. and Sigler, P.B., Cell , 99 (1999) 757.

44. Quiocho, F.A., Spulino, J.C. and Rodseth, L.E., Structure, 5 (1997) 997.

45. Sleigh, S.H., Seavers, P.R., Wilkinson, A.J., Ladbury, J.E. and Tame, J.R.H., J. Mol. Biol., 291 (1999) 393.

46. LaLonde, J.M., Bernlohr, D.A. and Banaszak, L.J., Biochemistry, 33 (1994) 4885.

47. Quiocho, F.A., Wilson, D.K. and Vyas, N.K., Nature, 340 (1989) 404.

48. Strynadka, N.C., Jensen, S.E., Johns, K., Blanchard, H., Page, M., Matagne, A., Frere, J.M. and James, M.N., Nature, 368 (1994) 657.

49. Delano, W.L., Ultsch, M.H., de Vos, A.M. and Wells, J.A., Science, 287 (2000) 1279.

50. Bogan, A.A. and Thorn, K.S., J. Mol. Biol., 280 (1998) 1.

51. Hu, Z., Ma, B., Wolfson, H. and Nussinov, R., Proteins, 39 (2000) 331.

52. Park, H., Bradrick, T.D. and Howell, E.E., Prot. Eng., 10 (1997) 1415.

53. Hamilton, J.B., Masters Thesis, University of TN (1997).

54. Strader, M.B., Smiley, R.D., Stinnett, L., VerBerkmoes, N.C. and Howell, E.E., Biochemistry, 40 (2001) 11344.

55. Smith, S.L. and Burchall, J.J., Proc. Natl. Acad. Sci. USA, 80 (1983) 4619.

56. Birdsall, B., Polshakov, V.I. and Feeney, J., Biochemistry, 39 (2000) 9819.

57. Adams, J., Johnson, K., Matthews, R. and Benkovic, S.J., Biochemistry, 28 (1989) 6611.

58. Wu, Y.D. and Houck, K.N., J. Am. Chem. Soc., 109 (1987) 2226.

59. Castillo, R., Andres, J. and Moliner, V., J. Am. Chem. Soc., 121 (1999) 12140.

60. Bystroff, C., Oatley, S.J. and Kraut, J., Biochemistry, 29 (1990) 3263.

61. Bruice, T.C. and Benkovic, S.J., Biochemistry, 39 (2000) 6267.

62. Reece, L.J., Nichols, R., Ogden, R.C. and Howell, E.E., Biochemistry, 30 (1991) 10895.

63. Dion-Schultz, A. and Howell, E.E., Prot. Eng., 10 (1997) 263.

64. Andres, J., Moliner, V., Safont, V.S., Domingo, L.R., Picher, M.T. and Krechl, J., Bioorg. Chem., 24 (1996) 10.

65. O'Brien, P.J. and Herschlag, D., Chem. Biol., 6 (1999) R91.

66. Babbitt, P.C. and Gerlt, J.A., J. Biol. Chem., 272 (1997) 30591.

67. Smithrud, D.B. and Benkovic, S.J., Curr. Opin. Biotech., 8 (1997) 459.

68. Mader, M.M. and Bartlett, P.A., Chem. Rev., 97 (1997) 1281.

69. Karlstrom, A., Zhong, G., Rader, C., Larsen, N.A., Heine, A., Fuller, R., List, B., Tanaka, F., Wilson, I.A., Barbas 3rd, C.F. and Lerner, R.A., Proc. Natl. Acad. Sci. USA, 97 (2000) 3878.

70. Connolly, M.L., J. Mol. Graphics, 11 (1993) 139.

Supplementary Materials

Table 1. List of predicted contacts for an NADPH conformer docked into R67 DHFR•Fol I using DOCK (the nicotinamide-ribose ring is *syn*; hydrogens not shown)

NADPH atom	Monomer, residue and atom	Distance in Ångstroms
adenine: AN7	A: T51 :OG1	3.47
nicotinamide ribose: NC5′	A: Q67 :CG	3.60
nicotinamide: O7	A: Q67: CD	3.49
nicotinamide: O7	A: Q67: OE1	3.09
nicotinamide ribose: NC2′	A: Q67: NE2	3.15
nicotinamide ribose: NO2′	A: Q67: NE2	3.43
nicotinamide ribose: NO5′	A: I68: O	2.99
PP$_i$: O3	A: I68: O	3.08
PP$_i$: P2	A: I68: O	3.48
nicotinamide ribose: NC5′	A: I68: O	3.43
PP$_i$: AO1	A: Y69: CD1	2.86
PP$_i$: AO2	A: Y69: CD1	3.14
PP$_i$: P1	A: Y69: CD1	3.29
PP$_i$: AO1	A: Y69: CE1	3.59
PP$_i$: AO2	A: Y69: CE1	2.88
adenine: AN6	B: G64: O	3.01
adenine: AC6	B: G64: O	3.18
adenine: AN1	B: G64: O	3.33
nicotinamide: NC5	C: V66: O	3.16
nicotinamide: NC5	C: V66: O	3.17
nicotinamide: N7	C: Q67: CG	3.47
nicotinamide: NC4	C: Q67: CG	3.41
nicotinamide: N7	C: Q67: CD	3.50
nicotinamide: NC4	C: Q67: CD	3.60
nicotinamide: NC7	C: Q67: CD	3.42
nicotinamide: NC3	C: Q67: CD	3.47
nicotinamide: NC4	C: Q67: OE1	3.56
nicotinamide: NC3	C: Q67: OE1	3.37
nicotinamide: N7	C: Q67: NE2	3.43
nicotinamide: NC7	C: Q67: NE2	3.47
adenine ribose: AO2	D: K32: CE	3.28
adenine ribose: AO1	D: K32: CE	2.88
adenine ribose: P	D: K32: CE	3.58
adenine ribose: AO2	D: K32: NZ	3.38
adenine ribose: AO1	D: K32: NZ	3.58
adenine: AC2	D: A36: CB	3.54
adenine: AN3	D: A36: CB	3.52
adenine ribose: AO1	D: Y69: CD1	3.12
adenine ribose: AO1	D: Y69: CE1	3.20

Table 2. List of Contacts for the Top Scoring Folate Conformer Docked into R67 DHFR•NMN using DOCK. Hydrogens are not explicitly shown. This conformer is one of several shown in Figure 5

Folate atom	Monomer, residue and atom	Distance in Ångstroms
pteridine: N8	B: Q67: CD	3.24
pteridine: C7	B: Q67: CD	3.46
pteridine: N8	B: Q67: OE1	3.43
pteridine: N8	B: Q67: NE2	3.52
pteridine: C7	B: Q67: NE2	3.33
Glu: O2	C: K32: CD	3.28
Glu: OE2	C: K32: CE	3.06
Glu: O2	C: K32: CE	3.60
Glu: O1	C: K32: CE	3.31
Glu: C	C: K32: CE	3.31
Glu: OE2	C: K32: NZ	3.58
Glu: O2	C: K32: NZ	3.52
Glu: O1	C: K32: NZ	3.20
Glu: C	C: K32: NZ	3.45
Glu: CG1	C: K32: NZ	3.59
Glu: O1	C: A36: CB	2.88
Glu: O2	C: Y69: CE1	3.13
Glu: O2	C: Y69: CZ	3.57
Glu: O2	C: Y69: OH	3.20
pteridine: N5	D: V66: O	3.52
pteridine: C4	D: Q67: CG	3.24
pteridine: O4	D: Q67: CG	3.59
pteridine: N3	D: Q67: CG	3.29
pteridine: C8A	D: Q67: CD	3.57
pteridine: C4A	D: Q67: CD	3.57
pteridine: C4A	D: Q67: OE1	3.52
pteridine: O4	D: I68: N	3.10
pteridine: O4	D: I68: CG1	3.34

Table 3. List of Contacts for Top Scoring DHF Conformer Docked into R67 DHFR•NMN (excluding hydrogens) using DOCK.

DHF Atom	Monomer, Residue and atom	Distance in Ångstroms
Glu: OE1	B: K32: NZ	3.03
Glu: OE1	B: S34: O	3.60
Glu: C	B: G35: CA	3.60
Glu: OE2	B: G35: CA	3.01
pteridine: N8	B: Q67: CD	3.60
pteridine: C7	B: Q67: NE2	3.30
pteridine: N8	B: Q67: NE2	3.56
Glu: O2	C: T51: OG1	2.91
pteridine: N10	C: I68: O	3.51
PABA: C13	C: I68: O	2.86
PABA: C14	C: I68: O	3.43
Glu: O2	C: P70: CG	3.48
PABA: C12	C: P70: CD	3.40
pteridine: N5	D: V66:O	3.20
pteridine: C6	D: V66:O	3.36
pteridine: O4	D: Q67: CA	3.53
pteridine: N3	D: Q67: CG	3.24
pteridine: C4	D: Q67: CG	3.48
pteridine: C2	D: Q67: CG	3.46
pteridine: N1	D: Q67: CD	3.56
pteridine: C8A	D: Q67: OE1	3.54
pteridine: O4	D: I68: N	2.90
pteridine: O4	D: I68:CG1	3.02